Accepted Manuscript

Synthesis, physicochemical properties, and biological activity of bile acids 3-glucuronides: Novel insights into bile acid signalling and detoxification

Serena Mostarda, Daniela Passeri, Andrea Carotti, Bruno Cerra, Carolina Colliva, Tiziana Benicchi, Antonio Macchiarulo, Roberto Pellicciari, Antimo Gioiello

PII: S0223-5234(17)31040-1

DOI: 10.1016/j.ejmech.2017.12.034

Reference: EJMECH 10012

To appear in: *European Journal of Medicinal Chemistry*

Received Date: 2 November 2017

Revised Date: 29 November 2017

Accepted Date: 11 December 2017

Please cite this article as: S. Mostarda, D. Passeri, A. Carotti, B. Cerra, C. Colliva, T. Benicchi, A. Macchiarulo, R. Pellicciari, A. Gioiello, Synthesis, physicochemical properties, and biological activity of bile acids 3-glucuronides: Novel insights into bile acid signalling and detoxification, *European Journal of Medicinal Chemistry* (2018), doi: 10.1016/j.ejmech.2017.12.034.

Graphical Abstract

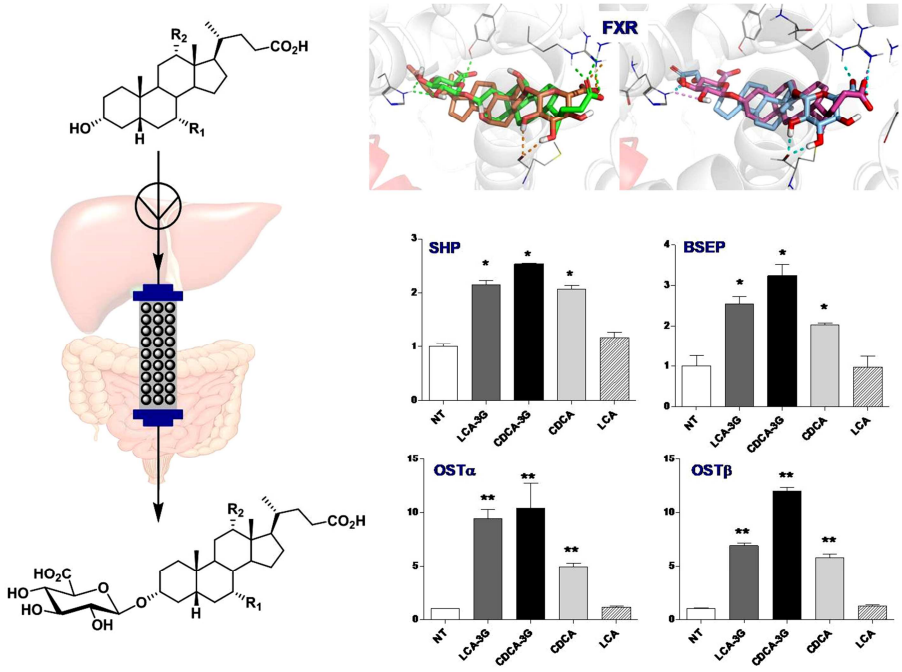

Synthesis, Physicochemical Properties, and Biological Activity of Bile Acids 3-Glucuronides: Novel Insights into Bile Acid Signalling and Detoxification

Serena Mostarda,[1] Daniela Passeri,[2,‡] Andrea Carotti,[1,‡] Bruno Cerra,[1] Carolina Colliva,[2] Tiziana Benicchi,[2] Antonio Macchiarulo,[1] Roberto Pellicciari,[2] and Antimo Gioiello[1,*]

[1] Department of Pharmaceutical Sciences, University of Perugia, Via del Liceo, 1, 06123 Perugia, Italy.

[2] TES Pharma, Corso Vannucci, 47, 06121 Perugia, Italy.

[‡] Equally contributed to the manuscript.

RECEIVED DATE (to be automatically inserted after your manuscript is accepted if required according to the journal that you are submitting your paper to)

*To whom correspondence should be addressed: Prof. Antimo Gioiello, Tel: +39.075.5852318; Fax: +39.075.5855160; E-mail: antimo.gioiello@unipg.it

Abstract

Glucuronidation is considered an important detoxification pathway of bile acids especially in cholestatic conditions. Glucuronides are less toxic than the parent free forms and are more easily excreted in urine. However, the pathophysiological significance of bile acid glucuronidation is still controversial and debated among the scientific community. Progress in this field has been strongly limited by the lack of appropriate methods for the preparation of pure glucuronides in the amount needed for biological and pharmacological studies. In this work, we have developed a new synthesis of bile acid C3-glucuronides enabling the convenient preparation of gram-scale quantities. The synthesized compounds have been characterized in terms of physicochemical properties and abilities to modulate key nuclear receptors including the farnesoid X receptor (FXR). In particular, we found that C3-glucuronides of chenodeoxycholic acid and lithocholic acid, respectively the most abundant and potentially cytotoxic species formed in patients affected by cholestasis, behave as FXR agonists and positively regulate the gene expression of transporter proteins, the function of which is critical in human conditions related to imbalances of bile acid homeostasis.

Keywords

Bile acids

Farnesoid X receptor

Flow chemistry

Glucuronidation

Abbreviations

BA, Bile acids; bile acids C3-glucuronides (BA-3Gs); BPR, back pressure regulator; BESP, bile salt export pump; CA, cholic acid; CAR, constitutive androstane receptor; CDCA, chenodeoxycholic acid; FXR, Farnesoid X receptor; FXRE, Farnesoid X receptor element; LBD, ligand binding domain; LCA, lithocholic acid; LXR, Liver X receptor; MRP, multidrug resistance related protein; OST, organic salt transporter; PXR, Pregnane X receptor; UGT, uridine diphosphate glucuronyltransferase.

1. Introduction

Bile acids (BAs) are important acidic steroidal hormones that play a central role in the control of their own homeostasis, triglyceride and carbohydrate metabolism as well as energy expenditure [1-3]. This regulatory action of BAs is mainly mediated by the farnesoid X receptor (FXR), a member of the nuclear receptor superfamily mainly expressed in tissues within the enterohepatic circulation where it mediates adaptive responses to cholestasis and other insults to the liver and intestine. The primary BA chenodeoxycholic (CDCA, **1**) (Figure 1) is considered the endogenous ligand of FXR with a micromolar activity, while cholic acid (CA, **2**) and secondary BAs as lithocholic acid (LCA, **3**) and deoxycholic acid (DCA, **4**) are mostly inactive at physiological concentrations [4-6].

Produced in the liver from cholesterol, primary BAs **1** and **2** are secreted into the bile and delivered in the duodenum, where they facilitate the absorption of fats, liposoluble vitamins and cholesterol by forming micelles (Figure 1) [7]. Once in the terminal ileum, 95% of BAs are reabsorbed by passive diffusion and active transport into the portal vein, transported back to the liver and stored in the gallbladder until the next meal. During this enterohepatic circulation, BAs undergo several modifications, including bacteria-catalyzed 7α-dehydroxylation, *N*-acyl amidation with taurine and glycine, sulfation at the C3 position, *N*-acylglucosamination and glucuronidation (Figure 1) [7].

Most of these transformations are finely regulated to maintain a balanced BA circulation and malfunctions are often the cause of disorders especially in the gastro-intestinal tract. In particular, the glucuronidation process consists in the transfer of the glucuronyl moiety from the co-substrate uridine-5'-diphospho-α-D-glucuronic acid to the BA scaffold [8]. The reaction promoted by uridine diphosphate glucuronyltransferases (UGTs) [9] generates BA metabolites as C3- and C24-glucuronides that are less toxic and more prone to be excreted with respect to the free parent compounds [10]. Besides the increased solubility in biological fluids, glucuronides are recognized by specific transporters such as the multidrug resistance related protein 3 (MRP3), that enable their secretion into blood and the subsequent urinary excretion [8,11,12]. Although in humans it is

considered a minor pathway for BA metabolism under normal physiological conditions [13], some evidence suggests that glucuronidation may become more relevant under cholestatic conditions, when the reduction of bile flow leads to BA accumulation and liver damage [8,10,14,15]. Glucuronidation is thus considered a protective route against BA hepatoxicity and BA-conjugating UGT enzymes have been proposed as targets for the treatment of cholestasis [16]. So far, BA C3-glucuronides (BA-3Gs) have been poorly investigated and their pathophysiological relevance is still controversial and debated [13]. This was also due to the lack of availability of authentic reference standards; indeed, conventional methods for their preparation [17-19] suffer from several drawbacks limiting their availability for biological and pharmacological studies. Indeed, while current enzymatic and extractive methods remain elusive, chemical syntheses are characterized by protection–deprotection steps of hydroxy groups at C7 and C12 positions, low yields, drastic reaction conditions, long reaction times and tedious purifications.

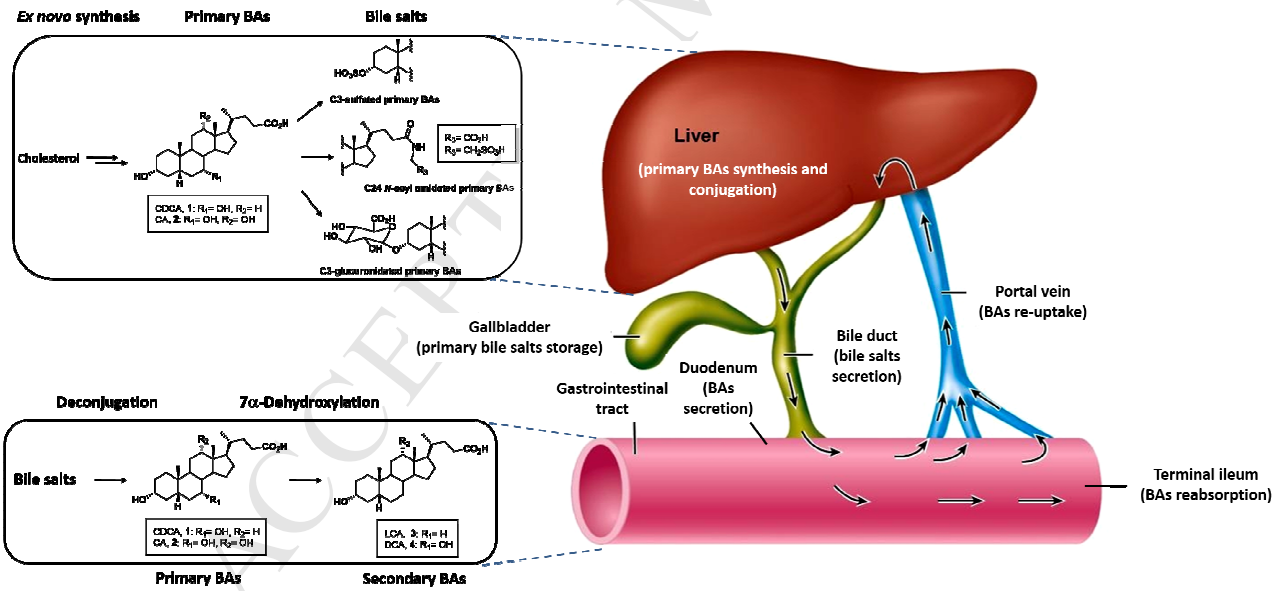

Figure 1. Enterohepatic circulation and metabolism of bile acids.

In this work, we report a novel and innovative synthesis of BA-3Gs based on the combined use of the continuous flow system and batch reactor. The synthesized compounds were characterized in

terms of physicochemical properties and tested for their ability to bind and activate the FXR receptor. We found that glucuronides of CDCA (CDCA-3G) and lithocholic acid (LCA-3G) were active at FXR with an efficacy comparable to the endogenous ligand CDCA, while they were not able to modulate other BA-responsive receptors. Binding modes of BA-3Gs to the ligand binding domain (LBD) of FXR have then been investigated using a computational protocol composed by induced fit docking and molecular dynamic (MD) simulations. Overall, results are discussed in terms of physio-pathological relevance along with FXR target gene expression.

2. Results

2.1 Combined flow/batch synthesis

The synthesis of BA-3Gs (**9**-**12**) was based on the in-flow conjugation of BA benzyl esters **5**-**8** by Koenigs-Knorr reaction followed by alkali hydrolysis performed under batch conditions (Scheme 1) [20]. Thus, BAs **1**-**4** were refluxed with benzyl bromide in the presence of Cs_2CO_3 in CH_3CN to furnish the desired esters **5**-**8** in high yields. Next, flow reactions were conducted in a flow mesoreactor system equipped with two pumps, an Omnifit PEEK column fixed in a reactor heater, a back pressure regulator (BPR) and a UV detector useful to check the reaction output. Thus, a solution of benzyl ester derivatives **5**-**8** (0.2 mmol, 0.1 M) and methyl 2,3,4-tri-*O*-acetyl-α-*D*-glucopyranosyluronate bromide (**13**, 2.6 equiv.) in toluene were pumped at 0.16 mL min^{-1} through the tubular reactor pre-packed with Fetizon's reagent (28% loading, Ag_2CO_3 5 equiv.) and molecular sieves (1:1, w/w) and thermostatted at 38 °C. The outflow was monitored by UV detector, collected in a beaker and stirred at r.t. for 1 h with a solution of NaOH (20 equiv., 10% w) in MeOH/H_2O (8:2, v/v). After concentration under reduced pressure, the aqueous phase was washed with Et_2O, acidified and purified by reverse flash chromatography. The desired BA-3Gs **9**-**12** were obtained in good overall yields and high purity grade.

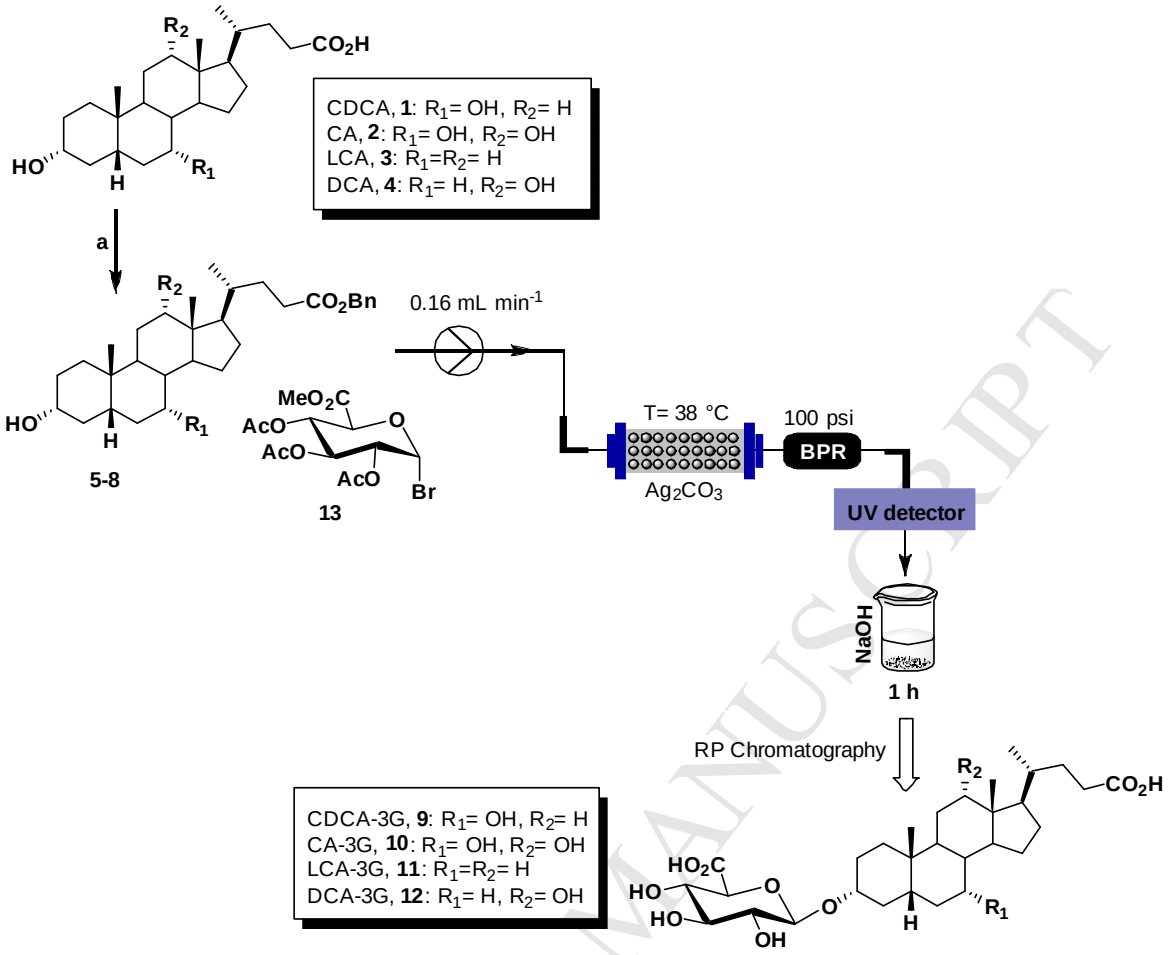

Scheme 1. General scheme used for the synthesis of bile acids C3-glucuronides. *Reaction conditions:* bile acid esterification: benzyl bromide, Cs_2CO_3, CH_3CN, reflux; in-flow Koenigs-Knorr reaction: Fetizon's reagent (28% loading), molecular sieves, methyl 2,3,4-tri-*O*-acetyl-α-*D*-glucopyranosyluronate bromide (**13**), toluene; hydrolysis: NaOH, MeOH, H_2O.

2.2 Physicochemical properties

The physicochemical properties of **9-12** were determined by HPLC-ESI-MS^2 using CDCA (**1**) as reference compound (Table 1). At physiological value of pH= 7.4, all BA-3G **9-12** were very soluble (≥300 μM) being in the ionized form (Table 1). At acidic pH (<1), the solubility of the compounds decreased following the order of the unconjugated compounds [21] with the exception of CA-3G (**10**) that was still highly soluble.

Table 1. Physicochemical properties of bile acid 3-glucuronides and CDCA.

Bile Acid	PBS Solubility (pH= 7.4, μM)[a]	HCl Solubility (pH= 1, μM)[a]	LogP $_{O/PBS}$ (pH= 7.4)[b]	LogP $_{O/HCl}$ (pH= 1)[b]	Albumin Binding (%)[c]
CDCA (**1**)	282.0 ± 4.2	33.0 ± 0.0	2.5 ± 0.0	2.5 ± 0.1	98.5 ± 0.2
CDCA-3G (**9**)	≥300	191.5 ± 7.8	-1.5 ± 0.1	2.5 ± 0.0	97.4 ± 0.3
CA-3G (**10**)	≥300	≥300	-1.2 ± 0.2	1.3 ± 0.1	53.6 ± 1.9
LCA-3G (**11**)	≥300	6.1 ± 0.3	-0.1 ± 0.1	1.5 ± 0.1	99.7 ± 0.1
DCA-3G (**12**)	≥300	211.5 ± 3.5	-1.7 ± 0.1	2.2 ± 0.0	87.0 ± 0.5

[a] Compounds were tested at 300 μM and 25 °C; [b] Compounds were tested at 1 μM; [c] BSA (4.5%) binding values were determined at 37 °C, in PBS aqueous buffer (pH= 7.4) and 10 μM concentration.

As the lipophilicity index, the partition-distribution coefficient LogP was calculated using a conventional shake flask procedure, by means of an equilibrium distribution of the molecule at a given pH between two phases, consisting of an aqueous buffer and 1-octanol (O) [22]. Since 1-octanol mimics the behaviour of lipid components of cellular membranes, this *in vitro* distribution simulates the *in vivo* repartition of BA-3Gs between the luminal or cytosolic compartment of living cells and their membranes. Typically, the higher the LogP value, the better the ability for the compound to cross the cellular membrane by passive diffusion. At physiological pH (7.4), BA-3Gs were characterized by negative $LogP_{O/PBS}$ as water-soluble double-charged species implying the need of transporters to pass the membrane [11,12], while at acidic contents a passive diffusion could not be excluded according to positive $LogP_{O/HCl}$ values (Table 1).

The binding of BAs to serum albumin is primarily driven by electrostatic interactions through the negatively charged carboxylic group of BA and hydrophobic contact with the steroidal body [23]. Accordingly, negligible differences in terms of bovine serum albumin affinity (BSA) measured by equilibrium dialysis at a fixed BA-albumin ratio, were observed between BA-3Gs **9-12** and CDCA (**1**), with the exception of the trihydroxylated CA-3G (**10**) that was poorly bound to the enzyme (Table 1). Moreover, the percentages of albumin binding were similar among the compounds,

suggesting a comparable unbound fraction in the plasma compartment and rates of hepatic clearance [23,24].

2.3 FXR activity and putative binding mode

The synthesized BA-3G **9-12** were evaluated for their ability to bind FXR using the AlphaScreen coactivator recruitment assay (Table 2). While most of the BA-3Gs had EC_{50} values at FXR comparable to their corresponding aglycone (parent) forms, surprisingly the glucuronidation of LCA (**3**) was effective in making the compound more active at FXR with an EC_{50} of 15 μM.

Table 2. FXR activity of natural bile acids and corresponding 3-glucuronides.

Bile Acid	**AlphaScreen Assay *h*FXR**	
	EC_{50} (μM)	**Efficacy (%)[a]**
CDCA (**1**)	15±5	100±2
CDCA-3G (**9**)	8±3	110±4
CA (**2**)	45±5	2.4±0.4
CA-3G (**10**)	91.5±8.5	14±1
LCA (**3**)	>100	-
LCA-3G (**11**)	15±5	68±8
DCA (**4**)	45±5	7±0.2
DCA-3G (**12**)	76±1	7±0.7

[a] Values calculated versus 50 μM CDCA (**1**).

The comparative FXR binding data obtained were further analyzed by means of computational modelling. In particular, a docking and MD protocol was applied to CDCA-3G (**9**) and LCA-3G (**11**). The LBD crystal of human FXR in complex with the endogen ligand CDCA (**1**) was retrieved from the Protein Data Bank (pdb code: 4QE6) [25] and used as starting structure for the computational study. The docking poses recorded for CDCA-3G (**9**) and LCA-3G (**11**) highlighted

two possible orientations of the BA scaffold: one with the carboxylic group at the C24 position interacting with the Arg331 as previously observed for all the FXR X-rays in complex with BAs (pdb codes 4QE6, 1OT7 and 1OSV) [25,26], called the 'head disposition', and another one ('tail disposition') with the core of the molecule flipped with the carboxylic moiety of the glucuronic portion now interacting with Arg331 (Figure 2).

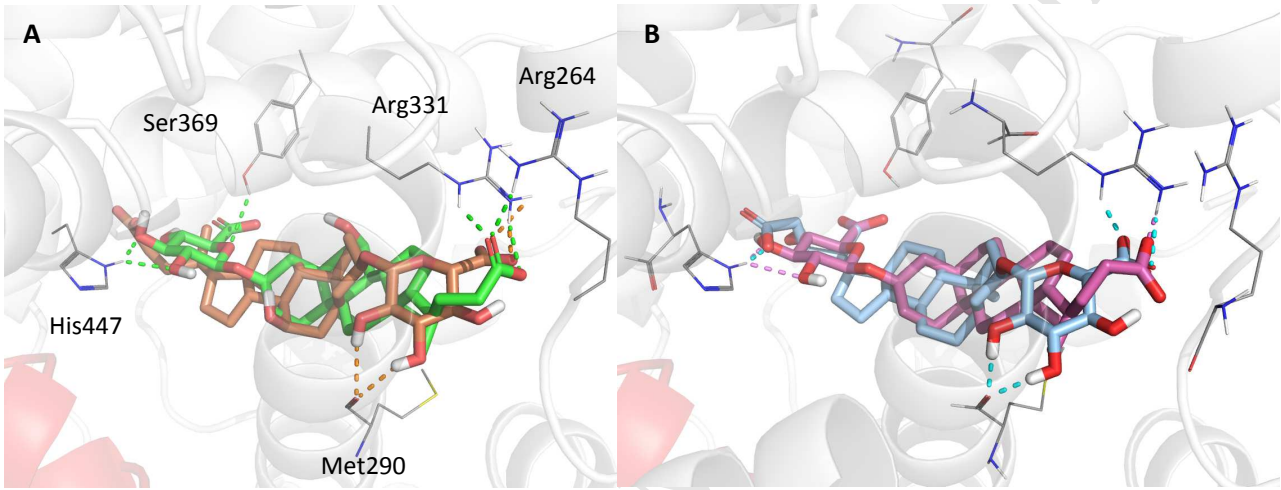

Figure 2. FXR putative docking poses of CDCA-3G (**9**) (**A**) and LCA-3G (**11**) (**B**). The 4QE6 X-ray FXR receptor is shown in white cartoon and the helix 12 is colored in red. The hydrogen bonds are displayed with dashed lines and the interacting residues are reported in lines and labeled. (**A**) CDCA-3G (**9**) is shown in green and orange sticks for the head and tail dispositions respectively. (**B**) LCA-3G (**11**) is shown in pink and cyan sticks for the head and tail pose respectively.

In order to gain insights into the most probable orientation, both head and tail complexes of CDCA-3G (**9**) and LCA-3G (**11**) were submitted to a 100 ns of MD together with the parent free BAs as reference compounds. Interestingly, the analysis of the stability of the compounds inside the binding site by means of the Root Mean Square Fluctuation (RMSF) of the heavy atoms of the molecules allowed us to identify the 'head orientation' as the most stable for both glucuronides (Figure 3). In particular, for the CDCA (**1**) graph it was possible to note that the CDCA-3G (**9**) head scaffold atoms (numbers 1-28) displayed lower values than the one recorded for CDCA (**1**), in line

with their biological activity (8 vs 15 μM, Table 2). The same trend was even more pronounced in the LCA (**3**) graph, where the LCA (**3**) RMSF scaffold atoms values (numbers 1-26) were often higher than the LCA-3G (**11**) ones. It is also worth noting that in both BAs scaffolds the glucuronic part was more stable when the head disposition was adopted (atom numbers over 28 for CDCA-3G (**9**) and over 26 for LCA-3G (**11**)) with respect to the tail pose.

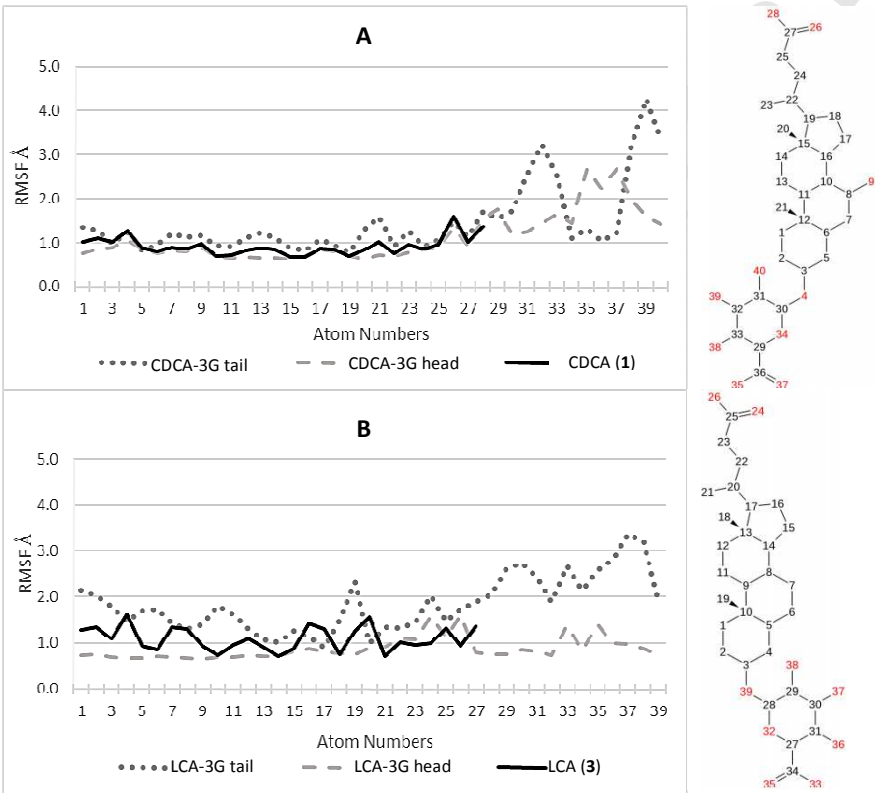

Figure 3. RMSF graphs of the CDCA-3G (**9**) (**A**) and LCA-3G (**11**) (**B**) molecular dynamic simulations in head and tail disposition, together with the parent BAs results. On the right, the 2D structure of the glucuronidated derivatives is also reported with atom numbering and color codes: red for oxygen and black for carbon atoms. The common atoms with the parent BAs are encoded by the same numbering.

Moreover, the stability of the interactions engaged during the molecular dynamics by the CDCA-3G (**9**) and LCA-3G (**11**) in head orientation (Figure 4) was slightly different among residues involved. In particular, the carboxylic moiety was interacting with equal stability with Arg331 in both cases,

and additionally with the Met265 backbone nitrogen and the Arg264 cationic head in the case of CDCA-3G (**9**) and LCA-3G (**11**), respectively.

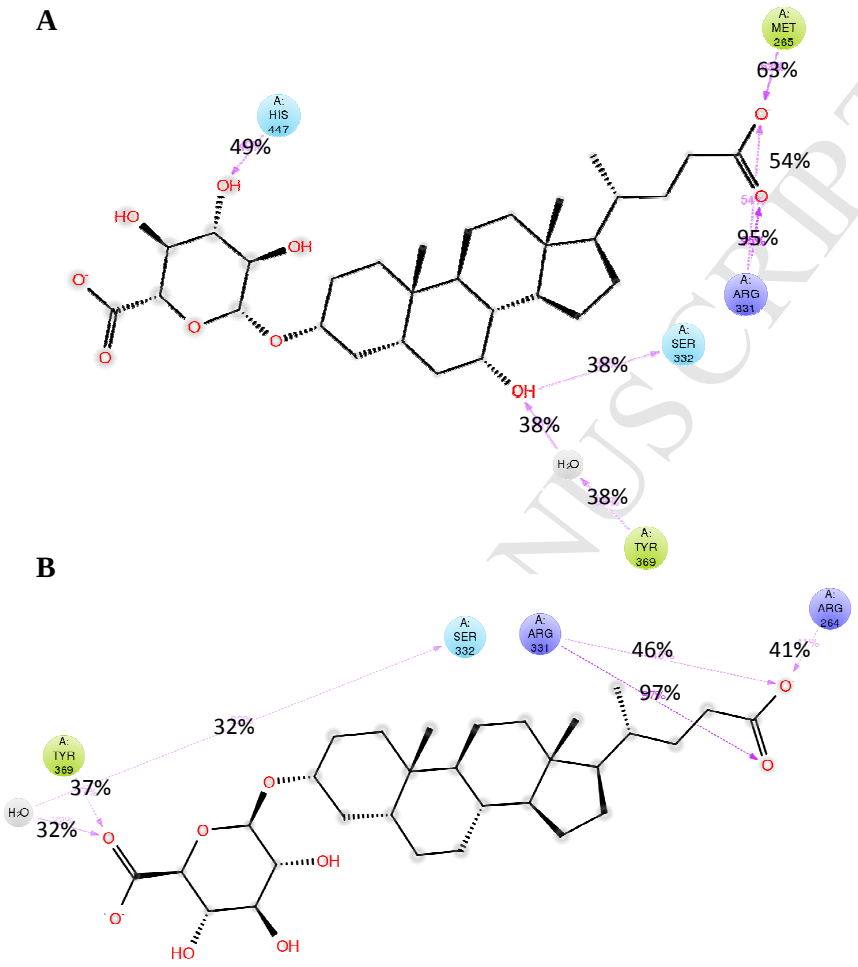

Figure 4. Ligand-protein interaction diagrams for CDCA-3G (**9**) (**A**) and LCA-3G (**11**) (**B**) molecular dynamics simulation in head orientation. Interaction strength is reported and quantified by the frequency of occurrences in the trajectory when a minimum percentage of 30% is achieved. The water molecules are shown in grey while the residues are labeled and colored in green, purple and cyan if hydrophobic, positively charged or polar respectively.

The OH in C7α position of CDCA-3G (**9**) formed a hydrogen bond with Ser332 and a water mediated interaction with Tyr369. Interestingly, in the case of LCA-3G (**11**) the same residues were involved in the interaction with the carboxylic moiety of the glucuronic portion thus

underlying a different binding mode adopted during the MD simulation with respect to the starting pose. Moreover, a hydroxyl group of the glucuronic moiety of the CDCA-3G (**9**) interacted with the His447, a residue located in the H11 that was involved through a t-shaped π-π stacking in the stabilization of the Trp469, an amino acid belonging to the H12. It is well known that H12 or AF-2 is directly involved in the coactivator recruitment process of FXR, an observation in line with the higher efficacy measured in the coactivator recruitment for the CDCA-3G (**9**) with respect to LCA-3G (**11**) (110% vs 68%, Table 2).

2.4 Biological and pharmacological activity of CDCA-3G and LCA-3G

Beside FXR, other nuclear receptors including the pregnane X receptor (PXR), the liver X receptor α (LXRα), the constitutive androstane receptor (CAR), and PPARs are shown to be involved in the detoxification and transport of BAs and their metabolites [27,28]. For this reason, we decided to evaluate the ability of CDCA-3G (**9**) and LCA-3G (**11**) to modulate these receptors using AlphaScreen assays. Results showed that neither CDCA-3G (**9**) nor LCA-3G (**11**) were able to bind the investigated receptors in both agonist and antagonist mode (*data not shown*).

Doses ranging from 1 to 100 μM of CDCA-3G (**9**) and LCA-3G (**11**) were then used to stimulate transiently transfected HEK293T cells and to evaluate FXR activation in cell-based assay (Figure 5). As expected, both compounds were able to activate FXR with an EC_{50} of 11 μM for CDCA-3G (**9**) and 35 μM for LCA-3G (**11**). In particular, LCA-3G (**11**) was shown to be less efficient than CDCA-3G (**9**) confirming what we observed in the AlphaScreen assay (Figure 5).

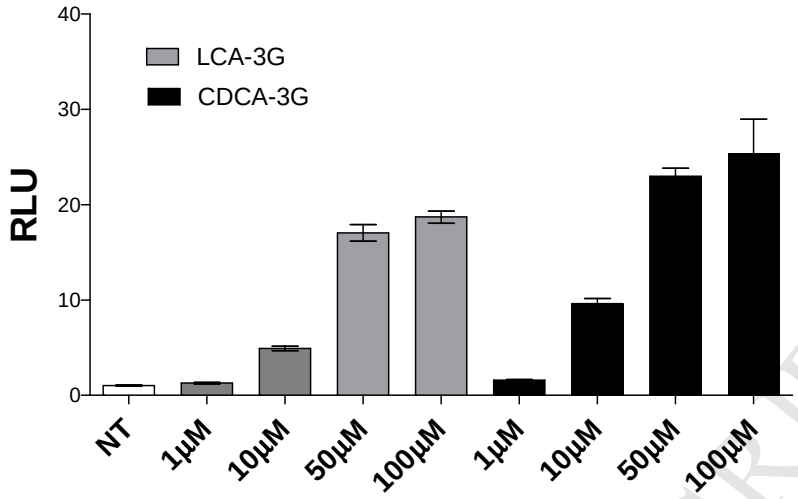

Figure 5. Transactivation assay on Hek293T by using FXR full length and the canonical FXRE (IR1) repeated three times upstream the luciferase gene. The results show a mean ±S.D. of two independent experiments performed.

The modulation of specific FXR genes involved in the detoxification of the liver was also explored. In particular, the effect of CDCA-3G (**9**) and LCA-3G (**11**) towards selected FXR target genes was determined by quantitative RT-PCR assays in HepG2 cells using CDCA (**1**) and LCA (**3**) as reference compounds (Figure 6). The results showed that both glucuronide compounds positively regulated BSEP, OSTα and OSTβ, with no apparent effect on the other transporters such as MDR1, MDR3, MRP1, MRP2, MRP4, MRP9, and ABCG5/8 gene (*data not shown*).

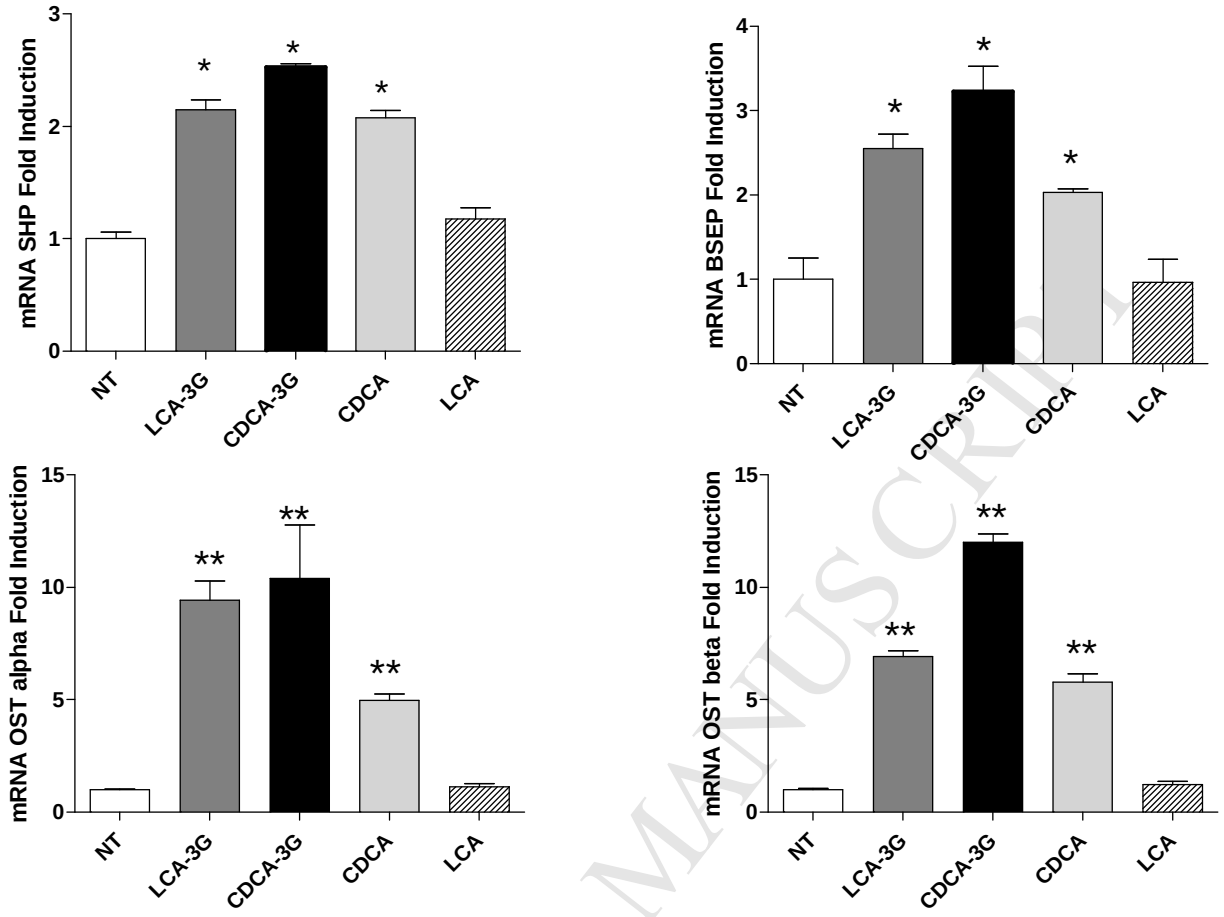

Figure 6. Real-time PCR analysis of mRNA expression of FXR target genes Shp, OSTα, OSTβ and BSEP in HepG2 cells treated with compounds LCA-3G (**11**), CDCA-3G (**9**), CDCA (**1**), and LCA (**3**) at 50 μM. * $p<0.05$ vs NT. ** $p<0.01$ vs NT

3. Discussion

Although glucuronidation of BAs is considered a major detoxification route in cholestatic conditions, its pathophysiological significance still remains to be completely defined [13]. This might be also due to the lack of reference standards and efficient methods for their preparation in adequate amount for *in vitro* and *in vivo* appraisals. In this paper, we report the set-up of a novel synthetic route to BA-3Gs **9-12** using flow technology. By this method, BA-3G can be prepared in

good overall yield and with a high degree of regioselectivity, providing quantities enabling their characterization in terms of physicochemical properties and biological activity.

Thus, we found that at physiological value of pH=7.4 BAs-3Gs **9**-**12** existed as very soluble double-charged molecular species (Table 1), as expected for endogenous metabolites destined for elimination routes [29,30]. They were also characterized by negative values of $LogP_{O/PBS}$ thus implying they need transporters to cross cellular membranes [11-12]. However, a passive absorption could not be excluded in acidic compartments; the increased aqueous solubility in acidic medium and the positive value of $LogP_{O/HCl}$ may suggest a plausible passive distribution. The microclimate pH at the membrane aqueous interface is appreciably lower than the intestinal bulk pH and could facilitate the formation of protonated species [31,32]. Among serum proteins, BAs exhibit the greatest affinity towards the most abundant human albumin and their binding values are known to decrease after *N*-acylamidation with taurine and glycine as by the introduction of polar hydroxy groups on the steroidal backbone [23]. Consistent with these observations, it emerged from our data that the C3-glucuronidation of BAs only slightly affected the albumin binding affinity when compared the unconjugated forms, thus confirming the carboxylic group at the BA side chain and the number of hydroxyl groups at the steroidal core as the main determinant for the albumin binding. From a physiological point of view, the binding of BAs to albumin strongly influences their circulating levels, determining both the unbound fraction and the rate of hepatic clearance from portal blood [23,24]. Particularly, the hepatic extraction efficiency results to be inversely correlated to the extent of BA binding to serum albumin [24,33,34]. Although the relative rate constants should be determined, it can be speculated a less efficient biliary secretion for BA-3Gs with respect to their corresponding *N*-acylamidated BAs, in favour of spill over into the systemic circulation.

The synthesized BA-3Gs **9**-**12** were then tested for their ability to bind and activate the FXR receptor, the key player involved in the regulation of BA homeostasis and detoxification. Previous findings show that CDCA-24G failed to activate FXR in FXRE reporter construct in UGT1A3-

HEK293 cell lines, suggesting that glucuronidation is a possible inactivating pathway for BAs [35]. Surprisingly, we found that both CDCA-3G (**9**) and LCA-3G (**11**) were active at FXR in a μM range of potency in both a cell-free (Table 2) and a cell-based assay (Figure 5). This result was rationalized by computational modelling studies and, in our opinion, is of great significance from a patho-physiological point of view. Indeed, the concentration of CDCA-3G (**9**) and LCA-3G (**11**) were reported to increase in cholestatic individuals [36]. It is postulated, that during cholestasis, an organism responds by transforming BAs into the respective 3-glucuronides that are less toxic, more prone to be secreted in urine and eliminated. Remarkably, according to our results, BA-3Gs are also endowed with the ability to stimulate FXR functions in protecting liver from insults and malfunctions. As mentioned, glucuronidation makes LCA less toxic and also active at FXR, protecting the liver from its accumulation as observed in cholestatic conditions. In line with this observation, both CDCA-3G (**9**) and LCA-3G (**11**) upregulate the gene expression of BSEP and OST-α and -β, which are crucial transporters involved in balancing BA homeostasis. While BSEP facilitates the excretion of BAs from the liver, OST-α and -β improve glucuronide secretion into the blood to be then excreted by kidney in the urine and, at the same time, their secretion into bile and elimination through faeces. Notably, both of these paths are more regulated by 3-glucuronides than by the endogenous FXR agonist CDCA (**1**).

In summary, we have described an innovative and efficient method for preparing BA-3Gs using continuous flow chemistry. The method allows preparing BA-3Gs on demand and according to the need. Moreover, we have provided for the first time a comprehensive and homogeneous physicochemical characterization of the major human BA-3Gs as well as their relative activity at FXR and other receptors involved in BA homeostasis and detoxification. In contrast to the C24 glucuronidation, our results suggest that the glucuronidation process at the C3 position for CDCA-3G and LCA-3G cannot be considered an inactivating process but rather a defensive mechanism played not only through the physicochemical properties of the resulting C3-glucuronides, but also

by the positive action at the FXR receptor. Although these findings need to be confirmed in animal models, overall this study provides new hypothesis and insights on the role of the glucuronidation in BA signalling.

5. Experimental Section

5.1 Synthetic chemistry

5.1.1 General method

^{1}H-NMR spectra were recorded at 400 MHz, and ^{13}C-NMR spectra were recorded at 100.6 MHz using the solvents indicated below. Chemical shifts are reported in ppm. The abbreviations used are as follows: s, singlet; d, doublet; dd, double doublet; t, triplet; m, multiplet; quint, quintet. All flow experiments were performed using a commercially available Vapourtec R2+/R4 module. TLC was performed on aluminum backed silica plates (silica gel 60 F254). Melting points were determined by the capillary method using a Buchi 535 instrument and they were not corrected. Benzyl esters (**5-8**) and methyl 2,3,4-tri-*O*-acetyl-α-*D*-glucopyranosyluronate bromide (**13**) were prepared as previously reported [20]. Mass spectroscopy was performed with a Dionex UltiMate 3000 HPLC separations module combined with a HCT ultra ion trap (Bruker). The analytical column was a Waters Xselect CSH Phenyl-Hexyl (5 μm, 2.1 × 150 mm), protected by a guard column 2.1 × 4 mm.

5.1.2 General method for the synthesis of C_3-glucuronidated bile acid derivatives

A toluene solution consisting of BA esters **5-8** (0.1 M) and methyl 2,3,4-tri-O-acetyl-α-*D*-glucopyranosyluronate bromide (**13**) (2.6 equiv.) was pumped at 0.16 mL min^{-1} through an Omnifit PEEK column (L × I.D. 150 mm × 6 mm) packed with Fetizon's reagent (28% loading, Ag_2CO_3 5 equiv.) and molecular sieves (4 Å, 325 mesh) (1 : 1, w/w). The reactor was warmed at 38 °C and fitted with a back pressure regulator (100 psi). The output was detected by UV, collected in a becker and stirred at r.t. for 1 h with a solution of NaOH (20 equiv., 10% w) in MeOH/H_2O (8:2,

v/v). After concentration under reduced pressure, the aqueous phase was firstly washed with Et_2O, then acidified with a solution of HCl 3 N up to pH 1 and purified by reverse flash chromatography using H_2O/MeOH as eluting solvent system. The desired BA-3Gs **9-12** were obtained in good overall yields and purity.

3α,7α-dihydroxy-5β-cholan-24-oic acid 3-β-*D*-glucuronide (**9**) was obtained in 95% yield as white solid (m.p.: 157 °C dec). ^{1}H NMR (400 MHz, CD_3OD): δ 0.70 (3H, s, 18-C*H*$_3$), 0.93 (3H, s, 19-C*H*$_3$), 0.97 (3H, d, *J*= 6.42 Hz, 21-C*H*$_3$), 3.19 (1H, *pseudo*-t, 2'-C*H*), 3.38 (1H, m, 3'-C*H*), 3.50 (1H, t, *J*= 9.65 Hz, 4'-C*H*), 3.52-3.64 (1H, m, 3-C*H*), 3.71 (1H, d, *J*= 9.67 Hz, 5'-C*H*), 3.80 (1H, s, 7-C*H*), 4.44 (1H, d, *J*= 7.71 Hz, 1'-C*H*). ^{13}C NMR (100.6 MHz, CD_3OD): δ 12.1, 18.8, 20.7, 21.8, 23.3, 24.6, 27.8, 29.2, 32.0, 32.3, 34.0, 35.8, 36.3, 36.7, 38.4, 40.7, 41.0, 43.1, 43.7, 51.5, 57.3, 69.0, 73.3, 74.8, 76.5, 77.5, 80.2, 102.2, 173.6, 178.1. HRMS(ESI)$^-$ m/z 567.4 [C26H43O5 (M - H)$^-$ requires 568.7].

3α,7α,12α-trihydroxy-5β-cholan-24-oic acid 3-β-*D*-glucuronide (**10**) was obtained in 90% yield as white solid (m.p. 141 °C dec). ^{1}H NMR (400 MHz, CD_3OD): δ 0.69 (3H, s, 18-C*H*$_3$), 0.89 (3H, s, 19-C*H*$_3$), 0.99 (3H, d, *J*= 6.26 Hz, 21-C*H*$_3$), 3.15 (1H, *pseudo*-t, 2'-C*H*), 3.36 (1H, t, *J*= 9.20 Hz, 3'-C*H*), 3.38 (1H, *pseudo*-q, 4'-C*H*), 3.52 (1H, d, *J*= 9.20 Hz, 5'-C*H*), 3.58-3.64 (1H, m, 3-C*H*), 3.77 (1H, s, 7-C*H*), 3.93 (1H, s, 12-C*H*), 4.37 (1H, d, *J*= 7.73 Hz, 1'-C*H*). ^{13}C NMR (100.6 MHz, CD_3OD): δ 11.0, 15.7, 21.1, 22.3, 25.5, 25.9, 26.7, 27.5, 30.8, 31.3, 33.8, 34.0, 34.2, 35.0, 36.4, 39.0, 41.0, 41.1, 45.5, 46.1, 67.1, 71.8, 72.0, 73.0, 74.2, 75.8, 77.7, 99.9, 174.9, 177.8. HRMS(ESI)$^-$ m/z 583.4 [C26H43O5 (M - H)$^-$ requires 584.7].

3α-hydroxy-5β-cholan-24-oic acid 3β-*D*-glucuronide (**11**) was obtained in 86% yield as white solid (m.p.: 167 °C dec). ^{1}H NMR (400 MHz, d^6-DMSO): δ 0.60 (3H, s, 18-C*H*$_3$), 0.85-0.92 (6H, m, 19-

C*H*$_3$ + 21-C*H*$_3$), 2.90 (1H, t, *J*= 8.16 Hz, 2'-C*H*), 3.13 (1H, t, *J*= 9.67 Hz, 3'-C*H*), 3.23 (1H, t, *J*= 9.11 Hz, 4'-C*H*), 3.28-3.38 (m, 2H, 3-C*H* + O*H* exchangeable proton), 3.48 (1H, d, *J*= 9.61 Hz, 5'-C*H*), 3.92-4.15 (1H, brs, O*H* exchangeable proton), 4.28 (1H, d, *J*= 7.76 Hz, 1'-C*H*), 4.86-5.02 (1H, brs, O*H* exchangeable proton). ^{13}C NMR (100.6 MHz, d^6-DMSO): δ 12.2, 18.5, 20.7, 23.5, 24.3, 26.5, 26.7, 27.1, 28.1, 30.7, 31.0, 34.2, 34.6 (2x), 35.0, 35.2, 35.7, 41.8, 42.6, 51.6, 55.8, 56.4, 72.1, 73.6, 75.5, 76.6, 77.4, 101.1, 172.6, 174.1. HRMS(ESI)$^-$ m/z 551.4 [C26H43O5 (M - H)$^-$ requires 552.7].

3α,12α-dihydroxy-5β-cholan-24-oic acid 3-β-*D*-glucuronide (**12**) was obtained in 85% yield as white solid (m.p.: 144 °C dec). ^{1}H NMR (400 MHz, CD_3OD): δ 0.72 (3H, s, 18-C*H*$_3$), 0.94 (3H, s, 19-C*H*$_3$), 1.01 (3H, d, *J*= 6.39 Hz, 21-C*H*$_3$), 3.20 (1H, *pseudo*-t, 2'-C*H*), 3.36-3.43 (1H, m, 3'-C*H*), 3.53 (1H, t, *J*= 9.10 Hz, 4'-C*H*), 3.66-3.72 (1H, m, 3-C*H*), 3.78 (1H, d, *J*= 9.73 Hz, 5'-C*H*), 3.96 (1H, s, 12-C*H*), 4.46 (1H, d, *J*= 7.74 Hz, 1'-C*H*). ^{13}C NMR (100.6 MHz, CD_3OD): δ 14.1, 18.5, 24.5, 25.8, 28.3, 28.5, 29.3, 29.5, 30.7, 31.7, 33.2, 35.7, 36.2, 36.3, 37.1, 37.6, 38.3, 44.5, 48.5, 49.0, 50.2, 74.1, 74.9, 75.7, 77.5, 78.4, 81.2, 103.4, 173.5, 179.1. HRMS(ESI)$^-$ m/z 567.4 [C26H43O5 (M - H)$^-$ requires 568.7].

5.2 Analytical methods

5.2.1 HPLC-ES-MS/MS method

Chemicals. All solvents were of high purity and used without further purification. Acetonitrile (MeCN) and MeOH from Biosolve® for ULC/MS; bovine serum albumins, ammonia solution 30%, glacial acetic acid and hydrochloric acid from Sigma Aldrich (Italy); Dulbecco's phosphate buffered saline w/Magnesium and Calcium (PBS) from EuroClone.

Instrumentation. Samples were analyzed using Dionex UltiMate 3000 HPLC separations module combined with a HCT ultra ion trap (BRUKER) using an electrospray interface. The analytical

column was a Waters Xselect CSH Phenyl-Hexyl 5 µm, 2.1 × 150 mm, protected by a guard column 2.1 ×4 mm. BAs were separated in elution gradient mode using 15 mM ammonium acetate buffer (pH= 8.0) as mobile phase A and MeCN/MeOH (75:25, v/v) as mobile phase B at a flow rate of 0.15 $mL \cdot min^{-1}$. Sample injection volume was 5 µL. The chromatotographic column was thermostated at 45 °C. The MS system was set with an electrospray ionization source (ES) in the negative mode with optimized parameters. Chromatograms were acquired using the mass spectrometer in multiple reaction monitoring (MRM) mode. QuantAnalysis (Bruker Daltonic) software version 1.8 was used for data acquisition and processing.

Sample preparation. Samples for water solubility (Ws), lipophilicity and albumin binding studies were brought to 25 °C and 37 °C and diluted 1:100 or 1:10 (v/v) with ammonium acetate buffer 15 mM pH 8 and MeCN/MeOH (75:25 v/v) in ratio 50:50 (v/v). The final solution was transferred to an autosampler vial and 5 µL was injected into the column.

Calibration curves. For each BA, stock solutions were prepared in MeCN/MeOH (1:1, v/v) at 1 mM and stored in screw cap disposable glass tubes at approximately -20 °C. Appropriate volumes of these stock solutions were further diluted with MeOH to obtain working solutions containing all the BAs studied in samples for physicochemical properties. A 6-point calibration curve (0.01 to 10 µM) was prepared by adding the appropriate amount of each corresponding BA working solution in mobile phase. Calibration curves were generated by plotting the peak area ratio of the respective compound *versus* the nominal concentration. The line of best fit was determined by linear-weighted ($1/x^2$) least-squares regression.

5.2.2 Physicochemical properties

Water solubility (Ws). Evaporate to dryness 300 µL of 1 mM stock solution in MeCN/MeOH (1:1, v/v) for each BA-3G and then resume with 1 mL of PBS solution at pH= 7.4 or with 1 mL of acid solution at pH= 1.0. Theoretical concentration in the solubility samples of BA were about 300 µM.

After 24 h under stirring at r.t., centrifuge (14.5 rpm for 20 min at 20 °C) the sample and dilute the sample (total dilution factor of 1:100 and 1:10, v/v). The dilution factor is dependent to the solubility of the compounds because for insoluble compounds a minor dilution to do for quantify using the linearity range and after inject 5 µL in HPLC-ES-MSMS. The solubility results were obtained by interpolating the signal of the sample in the calibration curve.

Lipophilicity (Log P). The 1-octanol/PBS and 1-octanol/HCl partition and distribution coefficient were evaluated using a conventional shake-flask procedure. The experiments were carried out using a BA concentration of 1 µM in solution buffered at pH= 7.4 (Dulbecco's phosphate buffered saline w/Magnesium and Calcium) or in acid solution at pH= 1.0 (HCl). The aqueous buffer (DPBS and acid solution) was previously pre-saturated with 1-octanol (0.30 mg of 1-octanol are dissolved in 1 L of water) like the 1-octanol was pre-saturated with buffer but before to prepare the solution centrifuge both octanol and buffer (2000 rpm for 5 min at 20 °C). The samples were left to equilibrate for 24 h under continuous stirring at r.t. (1-octanol/DPBS 50:50 and 1-octanol/HCl 50:50, v/v). After centrifugation (14.5 rpm for 20 min at 20 °C), the two phases were carefully separated by centrifugation. BA concentration in the water phase before and after partition in 1-octanol was measured by HPLC-ES-MS/MS.

Albumin binding. The extent of albumin binding was evaluated by equilibrium dialysis at a fixed BA-3G albumin ratio. Each BA-3G was dissolved at a concentration of 10 µM (2% DMSO) in 4.5% bovine serum albumin (BSA, fatty acid free from Sigma, St. Louis, MO)-PBS (pH= 7.4) and left to stand for 24 h at 37 °C. 4 mL of this solution were dialyzed in cellulose sacs with molecular weight cut-off of 12,000 to 14,000 Dalton (Spectra/Por, Spectrum Medicai lndustries lnc., Los Angeles, CA) against 10 mL of PBS (pH= 7.4). The system was equilibrated by gently shaking for 21 h at 37 °C. The BA concentrations of the dialyzed solution (corresponding to the free unbound

fraction) and of the starting solution were determined with HPLC-ESI-MS/MS under the same conditions as the previous analysis. The percentage of albumin binding was calculated as difference between the initial BA concentration and the unbound concentration in the dialyzed fraction.

5.3 Biology

5.3.1 FXR Alphascreen assay

Activity on FXR and other nuclear receptors was assayed by using Alphascreen technology in a coactivator recruitment assay. Anti-Glutathione S-transferase (GST)-coated acceptor beads were used to capture the GST-fusion FXR-ligand binding domain (LBD) whereas the biotinylated-Steroid Receptor Coactivator-1 (Src-1) peptide was captured by the streptavidin donor beads. Upon illumination at 680 nm, chemical energy is transferred from donor to acceptor beads across the complex streptavidin-Donor/Src-1-Biotin/GSTFXR-LBD/Anti-GST-Acceptor and a signal is produced. The assay was performed in white, low-volume, 384-well Optiplates (PerkinElmer) using a final volume of 25 μL containing final concentrations of 10 nM of purified GST-tagged FXR-LBD protein, 30 nM biotinylated Src-1 peptide, 20 $\mu g \cdot mL^{-1}$ anti-GST acceptor beads and 10 $\mu g \cdot mL^{-1}$ of streptavidin donor beads (PerkinElmer). The assay buffer contained 50 mM Tris (pH= 7.4), 50 mM KCl, 0.1% BSA and 1 mM dithiothreitol (DTT). The stimulation times with 1 μL of tested compound (solubilized in 100% DMSO) were fixed to 30 min at r.t.. After the addition of the detection mix (acceptor and donor beads) the plates were incubated in the dark for 4 h at r.t. and then were read in Envision microplate analyzer (PerkinElmer). Dose response curves were done in triplicate and Z'-factor was used to validate the assays. Non linear regression curves, without constraints, were performed by using four parameter equation and GraphPad Prism Software (GraphPad Inc.) to obtain the EC_{50} values.

5.3.2 Transactivation

Hek293T and HepG2 cell lines were from American Type Culture Collection (ATCC). Hek293T were maintained in DMEM/High Glucose (EuroClone) supplemented with 10% fetal bovine serum (EuroClone), 100 $U \cdot mL^{-1}$ penicillin, 100 $\mu g \cdot mL^{-1}$ streptomycin sulphate and 2 mM of glutamine (EuroClone). Human hepatoma HepG2 cell lines were maintained in minimum essential medium (MEM) supplemented with 10% FBS, 100 $U \cdot mL^{-1}$ penicillin, 100 $\mu g \cdot mL^{-1}$ streptomycin sulphate, 2 mM of glutamine, 100 μM non essential amino acids and 1 mM sodium pyruvate (EuroClone). Cells were grown at 37 °C in an atmosphere of 5% CO_2. Hek293T cells were transfected by using Fugene HD (Promega) in 100 μL of Optimem (Gibco) containing 100 ng pCMVSport4 FXR, 100 ng pSG5 RXR, 100 ng pGL4.74 (Promega) and 1000 ng of pGL4.23 (IR1)X3. After 24 h the cells were stimulated with a dose response of CDCA-3G (**9**) and LCA-3G (**11**) for an additional 18 h and then lysed to measure firefly luciferase activity. The experiments were normalized using renilla luciferase

5.3.3 Gene Expression

HepG2 cells were seeded at $6*10^5$ in a 6-well plate and treated for 18 h with CDCA-3G (**9**), LCA-3G (**11**), CDCA (**1**), LCA (**3**) at 50 μM. RNA was extracted using RNeasy Plus Kit (Quiagen) and 2 μg of cDNA was synthetized using 2 ug of RNA, 2.5 μM of random hexamers, RNaseOUT and SuperScript IV Reverse Transcriptase (Invitrogen Life Technologies) according to the manufacter's protocol.

50 ng of cDNA was used in a final volume of 20 μL containing SYBR Master Mix (Biorad) and 0.3 μM of the following primers:

Bsep for 5'-gcaatgcctctccttgtttgg-3' Bsep Rev 5'-acttgtaaccatcttctgacatgc-3'

Shp for 5'-atcctcttcaaccccgatgtg-3' Shp Rev 5'-acttcacacagcacccagtg-3'

Ostα for 5'-acccttttgccccatcaagag-3' Ostα Rev 5'-gcacacggcataaaacgagg-3'

Ostβ for 5'-ctgtggtggtcattataagcatgg-3' Ostβ Rev 5'-tctggtggctgcatcgtttc-3'

5.4 Computational Methods

All the calculations were performed with the Schrodinger Suite 2015-4 (Schrödinger Inc., NY, USA). The docked compounds were prepared with the default options of the *LigPrep* module to assign all the possible protonation states at pH= 7.0 ± 2. The crystal structure of FXR in complex with CDCA (**1**) (pdb code 4QE6) was used for docking experiments after being prepared with the standard options of the *Protein Preparation Wizard* protocol. The docking grid was calculated placing the coordinates of the center of mass of the co-crystallized ligand as center of a cubic box, having a side length of 10 Å. All docking calculations were performed using the single precision (SP) mode of Glide 6.9 [37]. The best poses were stored and used for MD simulations that were carried out with Desmond package [38]. In particular, the four resulting complexes were firstly solvated with water TIP3P and neutralized with the proper counterions using the system builder module. The box used was orthorhombic, having each side at a minimum distance of 10 Å from any atom of the complex. The force field used was the OPLS 2005 in an NPT (isothermic-isobaric) environment. The thermostat used was Berendsen type. The dynamic protocol was set in subsequent steps, with the first being a relaxing minimization, then a progressive increase of temperature to reach 300 Kin 140 ps, and finally a production run of 100 ns. Frames of the simulation were recorded every 5 ps. The MD trajectories were analyzed using the *Simulation Interaction Diagram* tool. The images were produced using PyMOL [39].

6. Acknowledgements

Intercept Pharmaceuticals (New York, USA) and TES Pharma (Perugia, Italy) are greatly acknowledged for their financial support. Thank also to Dr. Kevin Schaab (Intercept Pharmaceuticals) for manuscript revisions and useful discussions.

7. References and Notes

[1] F. G. Schaap, M. Trauner, P. L. Jensen. Bile acid receptors as targets for drug development. Nat. Rev. Gastroenterol. Hepatol. 11 (2014) 55-67.

[2] Y. Xu. Recent progress on bile acid receptor modulators for treatment of metabolic diseases. J. Med. Chem. 59 (2016), 6553-6579.

[3] A. Gioiello, B. Cerra, S. Mostarda, C. Guercini, R. Pellicciari, A. Macchiarulo. Bile acid derivatives as ligands of the Farnesoid X Receptor: molecular determinants for bile acid binding and receptor modulation. Curr. Top. Med. Chem. 14 (2014) 2159-2174.

[4] M. Makishima, A. Y. Okamoto, J. J. Repa, H. Tu, R. M. Learned, A. Luk, M. V. Hull, K. D. Lusting, D. J. Mangelsdorf, B. Shan. Identification of a nuclear receptor for bile acids. Science 284 (1999) 1362-1365.

[5] D. J. Parks, S. G. Blanchard, R. K. Bledsoe, T. G. Chandra, S. A. Kliewer, J. B. Stimmel, T. M. Wilson, A. M. Zavacki, D. D. Moore, J. M. Lehmann. Bile acids: natural ligands for an orphan nuclear receptor. Science 284 (1999) 1365-1368.

[6] H. Wang, J. Chen, K. Hollister, L. C. Sowers, B. M. Forman. Endogenous bile acids are ligands for the nuclear receptor FXR/BAR. Mol. Cell. 3 (1999) 543-553.

[7] A. F. Hofmann, L. R. Hagey. Bile acids: chemistry, pathochemistry, biology, pathobiology, and therapeutics. Cell. Mol. Life Sci. 65 (2008) 2461-2483.

[8] O. Barbier, J. Trottier, J. Kaeding, P. Caron, M. Verreault. Lipid-activated transcription factors control bile acid glucuronidation. Mol. Cell. Biochem. 326 (2009) 3-8.

[9] M. Ouzzine, L. Barré, P. Netter, J. Magdalou, S. Fournel-Gigleux. The human UDP-glucuronosyltransferases: structural aspects and drug glucuronidation. Drug Metab. Rev. 35 (2003) 287-303.

[10] M. Perreault, A. Bialek, J. Trottier, M. Verreault, P. Caron, P. Milkiewicz, O. Barbier. Role of glucuronidation for hepatic detoxification and urinary elimination of toxic bile acids during biliary obstruction. PLOS ONE 8 (2013) e80994.

[11] C. Pauli-Magnus, P. J. Meier. Hepatocellular transporters and cholestasis. J. Clin. Gastroenterol. 39 (2005) S103-S110.

[12] C. Pauli-Magnus, B. Stieger, Y. Meier, G. A. Kullak-Ublick, P. J. Meier. Enterohepatic transport of bile salts and genetics of cholestasis. J. Hepatol. 43 (2005) 342-357.

[13] A. F. Hofmann. Why bile acid glucuronidation is a minor pathway for conjugation of endogenous bile acids in man. Hepatol. 45 (2007) 1083-1084.

[14] H. Takikawa, H. Otsuka, T. Beppu, Y. Seyama, T. Yamakawa. Serum concentrations of bile acid glucuronides in hepatobiliary diseases. Digestion 27 (1983) 189-195.

[15] B. Almé, J. Sjovall. Analysis of bile acid glucuronides in urine. Identification of 3α,6α,12α-trihydroxy-5β-cholanoic acid. J. Steroid Biochem. 13 (1980) 907-916.

[16] J. Trottier, P. Milkiewicz, J. Kaeding, M. Verreault, O. Barbier. Coordinate regulation of hepatic bile acid oxidation and conjugation by nuclear receptors. Mol. Pharm. 3 (2006) 212-222.

[17] T. Iida, S. Tazawa, Y. Ohshima, T. Niwa, J. Goto, T. Nambara. Analysis of conjugated bile acids in human biological fluids. Synthesis of hyodeoxycholic acid 3- and 6-glycosides and related compounds. Chem. Pharm. Bull. 42 (1994) 1479-1984.

[18] J. Goto, K. Suzaki, T. Nambara. Studies on analysis of bile acids. Preparation of 3-glucuronides of 7- and 12-oxo bile acids. Chem. Pharm. Bull. 30 (1982) 4422-4428.

[19] J. Goto, K. Suzaki, T. Nambara. Synthesis of 3-glucuronides of unconjugated and conjugated bile acids. Chem. Pharm. Bull. 28 (1980) 1258-1264.

[20] S. Mostarda, P. Filipponi, R. Sardella, F. Venturoni, B. Natalini, R. Pellicciari, A. Gioiello. Glucuronidation of bile acids under flow conditions: design of experiments and Koenigs-Knorr reaction optimization. Org. Biomol. Chem. 12 (2014) 9592-9600.

[21] A. Fini, A. Roda, R. Fugazza, B. Grigolo. Chemical properties of bile acids. III. Bile acid structure and their solubility in water. J. Sol. Chem. 8 (1985) 595-603.

[22] A. Roda, A. Minutello, M. A. Angellotti, A. Fini. Bile acid structure-activity relationship: evaluation of bile acid lipophilicity using 1-octanol/water partition coefficient and reverse phase HPLC. J. Lipid Res. 31 (1990) 1433-1443.

[23] A. Roda, G. Cappelleri, R. Aldini, E. Roda, L. Barbara. Quantitative aspects of the interaction of bile acids with human serum albumin. J. Lipid Res. 23 (1982) 490-495.

[24] R. Aldini, A. Roda, A. M. Labate, G. Cappelleri, E. Roda, L. Barbara. Hepatic bile acid uptake: effect of conjugation, hydroxyl and keto groups, and albumin binding. J. Lipid Res. 23 (1982) 1167-1173.

[25] D. Kudlinzki, D. Merk, V. L. Linhard, K. Saxena, S. Sreeramulu, E. Nilsson, N. Dekker, L. Wissler, K. Bamberg, M. Schubert-Zsilavecz, H. Schwalbe, H. FXR with CDCA and NCoA-2 peptide. Manuscript to be published. DOI: 10.2210/pdb4qe6/pdb.

[26] L. Z. Mi, S. Devarakonda, J. M. Harp, Q. Han, R. Pellicciari, T. M. Willson, S. Khorasanizadeh, F. Rastinejad. Structural basis for bile acid binding and activation of the nuclear receptor FXR. Mol. Cell 11 (2003) 1093-1110.

[27] T. Claudel, G. Zollner, M. Wagner, M. Trauner. Role of nuclear receptors for bile acid metabolism, bile secretion, cholestasis, and gallstone disease. Biochim. Biophys. Acta 1812 (2011) 867-878.

[28] J. Y. Chiang. Bile acid regulation of hepatic physiology: III. Bile acids and nuclear receptors. Am. J. Physiol. Gastrointest. Liver Physiol. 284 (2003) G349-G356.

[29] A. Roda, A. Fini. Effect of nuclear hydroxy substituents on aqueous solubility and acidic strength of bile acids. Hepatology 4 (1984) 72S-76S.

[30] T. Farrell, L. Poquet, F. Dionisi, D. Barron, G. Williamson. Characterization of hydroxycinnamic acid glucuronide and sulfate conjugates by HPLC-DAD-MS^2: Enhancing chromatographic quantification and application in Caco-2 cell metabolism. J. Pharm. Biomed. Anal. 55 (2011) 1245-1254.

[31] H. Igimi, M. C. Carey. pH-Solubility relations of chenodeoxycholic and ursodeoxycholic acids: physical-chemical basis for dissimilar solution and membrane phenomena. J. Lipid Res. 21 (1980) 72-90.

[32] M. L. Lucas, J. A. Blair. The magnitude and distribution of the acid microclimate in proximal jejunum and its relation to luminal acidification. Proc. R. Soc. Lond. B 200 (1978) 27-41.

[33] T. Iga, C. D. Klaassen. Hepatic extraction of bile acids in rats. Biochem. Pharmacol. 31 (1982) 205-209.

[34] E. R. O'Maille, T. G. Richards, A. H. Short. The influence of conjugation of cholic acid on its uptake and secretion: hepatic extraction of taurocholate and cholate in the dog. J. Physiol. 189 (1987) 337-350.

[35] J. Trottier, M. Verreault, S. Grepper, D. Monté, J. Bélanger, J. Kaeding, P. Caron, T. T. Inaba, O. Barbier. Human UDP-glucuronosyltransferase (UGT)1A3 enzyme conjugates chenodeoxycholic acid in the liver. Hepatol. 44 (2006) 1158-1170.

[36] J. Trottier, M. Perreault, I. Rudkowska, C. Levy, A. Dallaire-Theroux, M. Verreault, P. Caron, B. Staels, M. C. Vohl, R. J. Straka, O. Barbier. Profiling serum bile acid glucuronides in humans: gender divergences, genetic determinants, and response to fenofibrate. Clin. Pharmacol Ther. 94 (2013) 533-543.

[37] R. A. Friesner, R. B. Murphy, M. P. Repasky, L. L. Frye, J. R. Greenwood, T. A. Halgren, P. C. Sanschagrin, D. T. Mainz. Extra precision glide: docking and scoring incorporating a model of hydrophobic enclosure for protein-ligand complexes. J. Med. Chem. 49 (2006) 7177-6196.

[38] K. J. Bowers, E. Chow, H. Xu, R. O. Dror, M. P. Eastwood, B. A. Gregersen, J. L. Klepeis, I. Kolossvary, M. A. Moraes, F. D. Sacerdoti, J. K. Salmon, Y. Shan, D. E. Shaw. Scalable algorithms for molecular dynamics simulations on commodity clusters. *Proceedings of the ACM/IEEE Conference on Supercomputing (SC06), Tampa, Florida*, **2006**, November 11-17.

[39] The PyMOL Molecular Graphics System, Version 1.8 Schrödinger, LLC.

Highlights

- A novel selective and gram scale synthesis of bile acids 3-glucuronides is provided.
- Bile acids 3-glucuronides exert a hepatoprotective action.
- CDCA-3G and LCA-3G behave as FXR ligands in in vitro assays.
- CDCA-3G and LCA-3G upregulate the gene expression of crucial transporter proteins.